

Estimating the fractal dimension: a comparative review and open source implementations

George Datseris,^{1, a)} Inga Kottlarz,^{2, 3} Anton P. Braun,^{2, 3} and Ulrich Parlitz^{3, 2}

¹⁾Max Planck Institute for Meteorology, 20146 Hamburg, Germany

²⁾Institute for the Dynamics of Complex Systems, University of Göttingen, Friedrich-Hund-Platz 1, 37077 Göttingen, Germany

³⁾Max Planck Institute for Dynamics and Self-Organization, Am Fassberg 17, 37077 Göttingen, Germany

(Dated: 17 December 2021)

The fractal dimension of state space sets is typically estimated via the scaling of either the generalized (Rényi) entropy or the correlation sum versus a size parameter. Motivated by the lack of quantitative and systematic comparisons of fractal dimension estimators in the literature, and also by new and improved methods for delay embedding, in this paper we provide a detailed and quantitative comparison for estimating the fractal dimension. We start with summarizing existing estimators and then perform an evaluation of these estimators, comparing their performance and precision using different data sets and taking into account the impact of features like length, noise, embedding dimension, non-stationarity, among many others. After comparing ten estimators, we conclude that for synthetic data the correlation based estimator is much better than the entropy one, while for real experimental data it seems to be the other way around. All other estimators perform worse. If the dynamic equations are known analytically, the Lyapunov dimension is always the most accurate. We furthermore discuss common pitfalls, like calculating the dimension of inappropriate data, automated ways to estimate the dimension, and provide an outlook of possible future research. All quantities discussed are implemented as performant and easy to use open source code via the software `DynamicalSystems.jl`.

When chaotic dynamical systems evolve in time, they (typically) create sets in the state space that have fractal properties. One of the major ways to characterize these chaotic sets is through a computationally feasible version of a fractal dimension. In the field of nonlinear dynamics, the correlation sum and the generalized (Rényi) entropy are the two most commonly used approaches. One attempts to find a scaling exponent of these quantities versus a size parameter, and this exponent approximates the fractal dimension. In the past few years researchers have calculated fractal dimensions for several diverse datasets. Here we provide a comprehensive, up to date and self-contained comparison of available methods for every conceivable scenario and provide open source implementations to compute each method.

I. INTRODUCTION

Fractal geometry deals with geometric objects (or sets) called *fractals*^{1,2}, that are “irregular” in terms of traditional Euclidean geometry. Their most striking property arguably is that they possess structure at all scales, which typically remains invariant in one form or another, no matter how much one zooms into the set. Because of this, the traditional topological dimension is not fit to describe these sets adequately. The concept of a *fractal dimension*, a generally non-integer number, is therefore employed to characterize such objects^{2,3}. The fractal dimension can be used to quantify the complexity

of the geometry, its scaling properties and self-similarity, and the effective ratio of surface areas to volumes².

The evolution of chaotic dynamical systems results in sets in the state space that are typically fractal³ and thus can be characterized by a fractal dimension^{4–10}, done to our knowledge for the first time by Russel & Ott¹¹. For dissipative systems, these sets are can be *strange* or *chaotic attractors*^{11,12} (boundaries of basins of attraction and chaotic saddles can also be fractal^{13,14}). For conservative systems they often have special properties and are (typically) called *fat fractals*¹⁵. For fractal sets resulting from evolving dynamical systems an estimate of fractal dimension provides some additional benefits. This is because this dimension counts the effective degrees of freedom of the time evolution, or even incorporates information regarding visitation frequency of parts of the chaotic set by the trajectory (the so-called *natural measure*)³. This means that calculating the fractal dimension for an experimentally obtained dataset can be used to guide the modelling process^{16,17}, as the ceiling of this number is the minimum number of independent variables that can model the system.

In this paper we are interested in computationally feasible ways to estimate the fractal dimension of a given trajectory, or dataset, originating from a stationary dynamical system. Our main operating assumption is that we do not know the dynamic rule (equations of motion) of the dynamical system the data are coming from. On the one hand this is motivated by the increase of interest in observed or measured multidimensional data, and higher accessibility of sensors and experimental data¹⁸. On the other hand, there is also noticeable recent progress regarding better attractor reconstruction techniques based on delay embeddings, which can also utilize multi-variate measurements, yielding a higher quality reconstruction overall, see¹⁹ and references therein.

Since the first review on the topic of the fractal dimen-

^{a)}Electronic mail: george.datseris@mpimet.mpg.de

sion by Theiler in 1990¹⁰, computers and software have improved and several new algorithms to estimate fractal dimensions have been proposed. It is thus timely to revisit the subject, and here we will provide a comparison and evaluation of fractal estimators across a range of topics much larger than what has been done so far. Beyond comparing and evaluating various fractal dimension estimators, we provide optimized, open source implementations for all algorithms discussed in this review as parts of the DynamicalSystems.jl software library²⁰ (see below).

This review and comparison paper is structured as follows. In Sect. II we discuss the current state of affairs and define the major methods we use to compute fractal dimensions. Connected with this section is Appendix A, which presents all (computationally feasible) algorithms we have found for estimating a fractal dimension. From there we decided the best methods to use for the paper core. This core is Sect. III. It presents the comparison and evaluation of the best methods to estimate a fractal dimension and highlights their drawbacks versus each other. We compare across data dimensionality, data length, different kinds of dynamical systems, noise levels, real world data, various embeddings of timeseries, the order q of the fractal dimension, among others. In Sect. IV we discuss potential pitfalls we encountered while implementing the methods ourselves but also from the literature review. We close the paper with a summary of our findings in Sect. V. Every result, plot, and method that we present in this paper is fully reproducible via open source code, see Appendix B for details.

II. STATE OF THE ART

An exceptional and accessible introduction and review regarding the fractal dimension was given by Theiler in 1990¹⁰. The theoretical background of the fractal dimension and the methods (known until 1990) to compute it are summarized, and a plethora of historic references is given there. Thus, here we focus on reviewing and comparing practical aspects for estimating fractal dimensions. A more recent publication on fractal dimensions in a style of a review by Lopes & Betrouni in 2009²¹. However, it is focused on image analysis and pattern recognition, and does not do any quantitative comparison. The most recent detailed source that provides quantitative information on the limitations and pitfalls of fractal dimension estimates is the well known textbook by Kantz & Schreiber¹⁶.

A number of ways to estimate a fractal dimension, that are applicable to dynamical systems, have been devised in the literature. For this comparison we found, implemented, and compared the methods that we briefly summarize in Table I. In the following, we assume that we have a set X that contains N D -dimensional points. We will use the letter Δ to denote various versions of the fractal dimension.

A. Entropy of natural density

The first way to define Δ is based on an approximation of the natural density¹⁵ of the set. By discretizing the state space in boxes of size ε one can assign an estimate of the probability $p_i, i = 1, \dots, M$ to each box, which is simply the count of points in the box divided by the total amount of points N . From these probabilities, the Rényi (also called generalized) entropy is defined as³³

$$H_q = \frac{1}{1-q} \log \left(\sum_{i=1}^M p_i^q \right). \quad (1)$$

For $q = 1$ it reduces to the known Shannon entropy while for $q = 0$ it becomes $\log(M)$ with M the minimum number of boxes needed to cover the set X . Several different algorithms have been suggested in the literature for estimating these probabilities p_i , see Appendix A. In the main comparison of Sect. III we will use the algorithm A 1 which works for any values of D, N, ε while having performance scaling of $D \cdot N \cdot \log(N)$, and which to our knowledge not been published before.

After obtaining H_q , its scaling versus ε can be used to define the so-called *generalized dimension* of order q ^{34,35}, done to our knowledge first time for $q = 1$ by Russel, Hanson and Ott¹¹

$$\Delta_q^{(H)} = \lim_{N \rightarrow \infty} \lim_{\varepsilon \rightarrow 0} \left(\frac{-H_q(\varepsilon)}{\log \varepsilon} \right). \quad (2)$$

Both limits are theoretical and cannot be realized in practice. As a result, $\Delta_q^{(H)}$ is estimated by plotting $-H_q$ vs. $\log(\varepsilon)$ and estimating the slope of a linear scaling region (for sufficiently large N , more on this in Sect. IV A). $\Delta_0^{(H)}$ is called the box-counting or capacity dimension, while $\Delta_1^{(H)}$ provides the information dimension.

If the fractal dimension depends on q , the set is called multi-fractal. This is the case when the natural measure underlying the attractor is non-uniform. Large positive values of q then put more emphasis on regions of the attractor with higher natural measure. In dynamical systems theory, almost all chaotic sets are multi-fractal⁸. The dependence of $\Delta_q^{(H)}$ on q is connected with another concept, the so-called singularity spectrum, or multifractality spectrum $f(\alpha)$, however we will not be calculating $f(\alpha)$ here and refer to other sources for more (see e.g. chapter 9 of Ref.¹² by Ott).

B. Correlation sum

The second way of defining a fractal dimension uses the correlation sum⁴. This sum, which can also be generalized to

Estimator	Description	Main Refs.
Natural measure entropy	Scaling of generalized entropy H of amplitude binning, versus box size	11
Molteno's histogram optimization	Optimized algorithm for amplitude binning with restricted size ε	22
Correlation sum	Logarithmic scaling of correlation sum versus box size	4,23
Box/prism-assisted correlation sum	Optimized algorithm to calculate the correlation sum	24
Performance-optimized box size	Optimized for performance box-assisted algorithm	25
Logarithmic correction	Better converging fit instead of the standard least square fit of $\log(C)$ vs. $\log(\varepsilon)$	26
Taken's estimator	Maximum likelihood estimation of scaling exponent, $C(\varepsilon) \propto \varepsilon^\Delta$ for $\varepsilon \in (0, \varepsilon_{\max}]$	7,27
Judd's estimator	Binned MLE with additional degrees of freedom from polynomial	28,29
Mean return times	Logarithmic scaling of mean return time to an ε -sphere, versus ε	10,30
Lyapunov dimension	Kaplan and Yorke's linear interpolation for sum of Lyapunov exponents = 0	31
Lyapunov dimension via fits	Higher-order interpolations and other fits for sum of Lyapunov exponents = 0	32

TABLE I: Description of various estimators for fractal dimension considered in this paper, see also Appendix A.

an order q , is given by^{5,16,23}

$$C_q(\varepsilon) = \left[\mathcal{N} \sum_{i=w+1}^{N-w} \left[\sum_{\substack{j=1 \\ |i-j|>w}}^N B(\|\mathbf{x}_i - \mathbf{x}_j\| < \varepsilon) \right]^{q-1} \right]^{1/(q-1)} \quad (3)$$

$$\mathcal{N} = \frac{1}{(N-2w)(N-2w-1)^{q-1}}$$

where $B(\cdot) = 1$ if its argument is true, 0 otherwise and $w \geq 0$ is the correction by Theiler³⁶ (Theiler window) which removes spurious correlations due to dense sampling of continuous dynamical systems. We choose w as follows: for each timeseries present in the multi-dimensional input data we calculate the first minimum of its self-mutual information. The maximum of these minima is w .

Originally the version explicitly having $q = 2$ was used to define the correlation dimension⁴, and the process of defining a generalized fractal dimension was in fact the same as in H_q for any q . A linear scaling region is estimated from the curve of $\log(C_q)$ versus $\log(\varepsilon)$. Then the correlation-sum-based fractal dimension $\Delta_q^{(C)}$ would be the slope of that linear region. We leverage two improvements here. First, to calculate $C(\varepsilon)$ we used a box-assisted method^{24,25}. We modify this method as discussed in App. A 4, because otherwise it fails for data with even a small amount of noise (see discussions in Sect. III F and App. A 4). Second, instead of a standard least squares fit $\log(C) \sim a + \Delta^{(C)} \log(\varepsilon)$, we used the correction by Sprott & Rowlands²⁶ when possible (i.e. when at least half the range has $\log(\varepsilon) < 0$). Ref.²⁶ optimizes the fit $\log(C) \sim a + \Delta^{(C)} \log(\varepsilon) + b \log(-\log(\varepsilon))$ (a, b are parameters to be optimized in parallel with $\Delta^{(C)}$). It is intended to give better fits for sets that have a slowly-converging fractal dimension estimate (see Sect. III B).

C. Lyapunov (Kaplan-Yorke) dimension

Another dimension estimate proposed by Kaplan and Yorke^{31,37} is based on the Lyapunov exponents characteriz-

ing an attractor. Let $\{\lambda_i\}$ denote the Lyapunov spectrum, with $\lambda_1 \geq \lambda_2 \geq \dots \geq \lambda_D$. Then the Lyapunov dimension is defined as

$$\Delta^{(L)} = \ell + \frac{\sum_{i=1}^{\ell} \lambda_i}{|\lambda_{\ell+1}|}, \quad \ell = \max_j \left[\sum_{i=1}^j \lambda_i > 0 \right]. \quad (4)$$

In simple terms, it is the (linearly interpolated) index value where the sum of the Lyapunov exponents of the set first crosses zero. Table II provides estimates for the systems we use in this paper. It is conjectured that $\Delta^{(L)} \approx \Delta_1^{(H)}$, see also³⁸, and generally one does find similar values in practice, however here we will revisit this conjecture in more detail. An extension to Eq. (4) has been proposed in³² that is not included in the main comparison but discussed in Appendix A. Keep in mind that Eq. (4) is defined only for dissipative systems, where $\sum \lambda_i < 0$. Applying it to conservative systems does not seem to make much sense. E.g., Hamiltonian systems satisfy $\lambda_i = -\lambda_{D-i+1}$ and obtain $\Delta^{(L)} = D$ always, even though the motion might happen in a lower-dimensional manifold. E.g., for the 4D Hénon-Heiles system (Fig. 2) energy conservation limits the dynamics in a 3D manifold, and thus its fractal dimension cannot be greater than 3.

$\Delta^{(L)}$ has a huge advantage when compared to the previous two definitions of fractal dimensions: it can be computed with high precision, even for high dimensional systems (where the other methods typically suffer from accuracy, as we will show below). But it also has a huge disadvantage: practically it can be computed only if the dynamic rule (equations of motion) is known. Only using the dynamical rule and its linearization one can estimate the entire Lyapunov spectrum with satisfactory precision, for example by means of the known algorithm due Shimada and Nagashima³⁹ and Benettin et al.⁴⁰. From a finite, and often noisy real world dataset, calculating the entire spectrum of exponents is a very challenging task that requires for higher dimensional attractors very large data sets⁴¹. Therefore one is in most case better off calculating H_q or C_q directly.

System	D	$\Delta^{(L)}$
Lorenz96	4	2.99
Lorenz96	6	4.93
Lorenz96	8	6.91
Lorenz96	10	8.59
Lorenz96	12	10.35
Lorenz96	14	12.10
Rössler (chaotic)	3	1.9
Hénon-Heiles (chaotic)	4	4 (3 is valid)
Hénon map	2	1.26
Towel map	3	2.24
Coupled logistic maps	8	8

TABLE II: Lyapunov (Kaplan-Yorke) dimensions for systems with known dynamic rule (see Table III).

III. DETAILED COMPARISONS

In this section we perform a quantitatively rigorous and exhaustive comparison of the methods based on entropy and correlation sum, using the Lyapunov dimension as a check. The motivation of choosing these methods is explained in Appendix A. Before any numerical analysis we normalize input data X so that each of its columns is transformed to have 0 mean and standard deviation of 1. This linear transformation leaves dynamic invariants (like the fractal dimension) unaffected, however makes all numerical methods more accurate and faster to converge.

In the following subsections all results will be presented with the same plot type, as e.g. shown in Fig. 1. The legend shows the different datasets used in the plot and a description of the plot's purpose. Top panel is entropy estimate while bottom is correlation sum. To estimate $\Delta^{(H)}, \Delta^{(C)}$, for each curve we identify automatically, and objectively, a linear scaling region as discussed in Sect. IV A. This region is denoted by markers of the same color on each curve. The secondary legends inside the panels provide the 5-95% confidence intervals for the estimated slopes of these segments. Unless otherwise stated, all datasets used have length $N = 10^5$ and continuous systems are sampled with approximately 10 points per characteristic oscillation period.

A. Benchmark sets with known dimensions

The best place to start is a simple sanity and accuracy test of the two main estimators for sets whose fractal dimension can be computed analytically in a straightforward manner. This is shown in Fig. 1. We use a periodic orbit from the Rössler system ($\Delta = 1$), a quasiperiodic orbit of order 2 from the Hénon-Heiles system ($\Delta = 2$), the Koch snowflake ($\Delta = \log(4)/\log(3) \approx 1.262$), the Kaplan-Yorke map ($\Delta = 1 - \log(2)/\log(0.2) \approx 1.4306$), a uniform filling of the 3D sphere ($\Delta = 3$) and a chaotic trajectory of the Standard Map (SM) for very high $k = 64$, which covers uniformly the state space and thus has $\Delta = 2$.

Some results that will be repeatedly seen throughout this

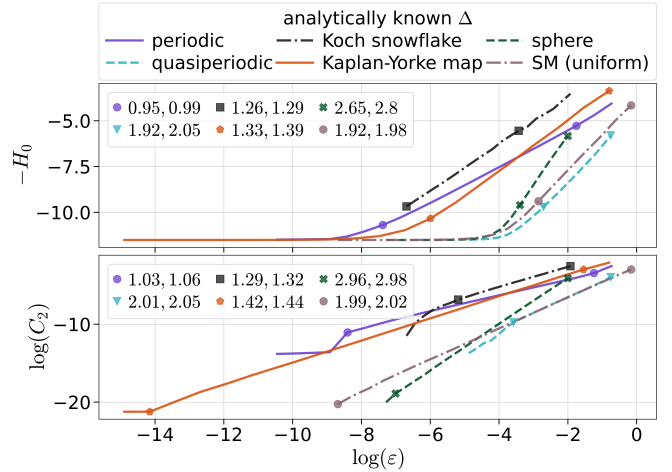


FIG. 1: Fractal dimension estimates for sets with analytically known fractal dimension. The figure title maps colors to set names. The legends within each axis map colors to two numbers which mean the (5%, 95%) confidence intervals corresponding to the estimation of the fractal dimension (curve slope). The markers on the curves denote the start and end of the estimated linear region.

paper become clear. The correlation sum method is more accurate for synthetic data for three reasons. First, its linear scaling region covers a wider range of ϵ values, while H saturates much more quickly to flatness for small ϵ . Notice that $\log(C)$ cannot saturate for small ϵ , but instead diverges to $-\infty$, but we can never reach this point due to the processes that chooses the appropriate overall range of ϵ (Sect. IV A). Both curves would in principle saturate to flatness for very large ϵ , specifically exceeding the set's total size, but we again do not reach this threshold based on the choice of the range of ϵ .

Second, within the linear scaling region the curves fluctuate less, resulting in a narrower confidence interval. Comparing confidence intervals is only meaningful if the same method is used to extract them. That is why specifically for Fig. 1 we used the standard least squares fit for $\log(C)$ instead of the aforementioned correction of Ref.²⁶. Third, the actual numbers we obtain for Δ from the correlation sum method are closer to the analytically expected values, than those of the entropy-based method. Especially for sets that should have an integer fractal dimension the correlation sum method is much closer to the actual result.

B. Different dynamical systems

In the following we cross-compare with the value obtained from the Lyapunov (Kaplan-Yorke) dimension which for all systems of interested used in this paper is found in Table II. In Fig. 2 we compare 3 discrete and 3 continuous dynamical systems of different input dimensionality (systems are defined in detail in App. C). We confirm the result of the previous section, i.e. the correlation sum method is more accurate than

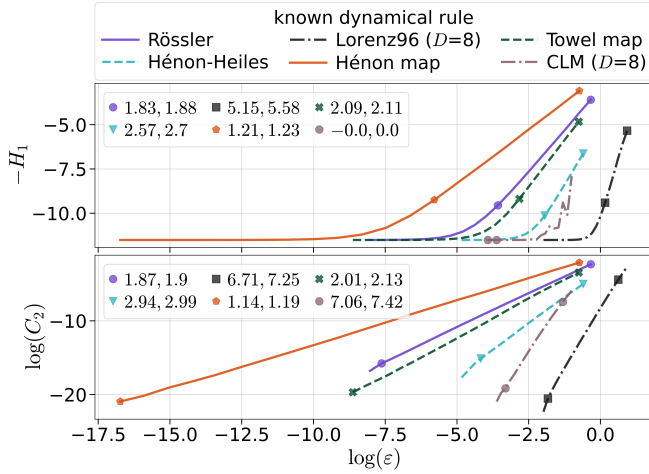


FIG. 2: Fractal dimension estimates for sets coming from different dynamical systems with known dynamical rule. CLM stands for Coupled Logistic Maps. We are not sure why CLM fails to yield a steady slope for H , but instead is jagged, but the focus of this paper is not individual systems so we leave this for further study.

the entropy one because it is much closer to the values expected from the Lyapunov dimension (Kaplan-Yorke conjecture). Furthermore, the entropy method seems to underestimate the fractal dimension more strongly as the state space dimensionality increases. This is expected given the fact that the entropy method works via a histogram approximation of the natural density, and it is well known that the higher dimensional the data, the less accurate binning them becomes.

This figure also allows us to indeed confirm that the correction by Sprott & Rowlands is impactful, especially for high-dimensional sets where the convergence is the slowest. For example, the standard linear regression fit would give confidence intervals (6.44, 6.6) for the 8-dimensional Lorenz96 model and (5.78, 6) for the 8 coupled logistic maps. These values are closer to the entropy based estimates but further away from the $\Delta^{(L)}$ estimates of Table II. While the logarithmic correction confidence intervals are larger, it is better to have more confidence that the true Δ is within the confidence interval, than to have a smaller confidence interval.

C. Amount of data points

Keeping the dimensionality and system type constant but varying length leads us to an interesting observation in Fig. 3. The entropy-based method performs poorly, if not horribly, for small N . What is astonishing is how robust is $\Delta^{(C)}$ versus the data length, where the plots show that it yields surprisingly good estimates for N as small as $N = 500$, with only small changes in the estimated Δ for decreasing N . This is even true for real-world experimental data (see Sect. III G for a description). Another interesting finding is that for ultra-small real world data the estimate seems to give *larger* $\Delta^{(C)}$ as

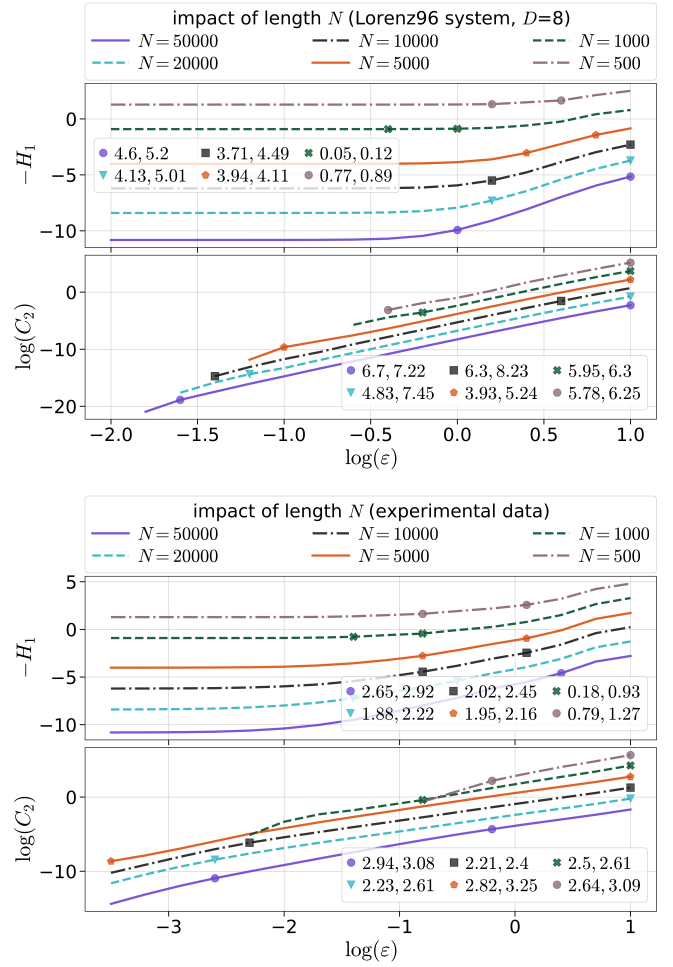


FIG. 3: Dependence of estimators on data length N . Bottom plot is using experimental dataset “electroch. 1” from Fig. 7. The curves have been vertically offset for visual clarity. For these plots we have used the automatic ϵ range estimated of Sect. IV A only for the largest datasets and use the same range for the rest. As a result $\log(C)$ cuts off to $-\infty$ as N decreases.

N decreases, while the current knowledge (see below) is that the dimension is *underestimated* for small data.

These findings beg the question of comparing with the known result of Eckmann and Ruelle⁴². They provide an argumentation that places strong limitations on estimates of fractal dimension from finite data⁴³. They argue that the algorithm producing $\Delta^{(C)}$ is upper bounded by the value

$$\Delta_{\max}^{(C)}(N) = \frac{2 \log N}{\log(1/\rho)}, \quad \rho = \frac{\epsilon_{\max}}{E} \quad (5)$$

with E the characteristic diameter of the chaotic attractor and $\epsilon_{\max} \ll E$ the maximum ϵ we fit the linear slope up to. Eckmann and Ruelle argue that $\rho < 0.1$, although in this work we use $\rho \approx 1/e^2$ as stated in Sect. IV A. This also highlights a “problem” with Eq. (5), as ρ cannot be decided uniquely and objectively from the data. Even with the estimate of $\rho = 0.1$,

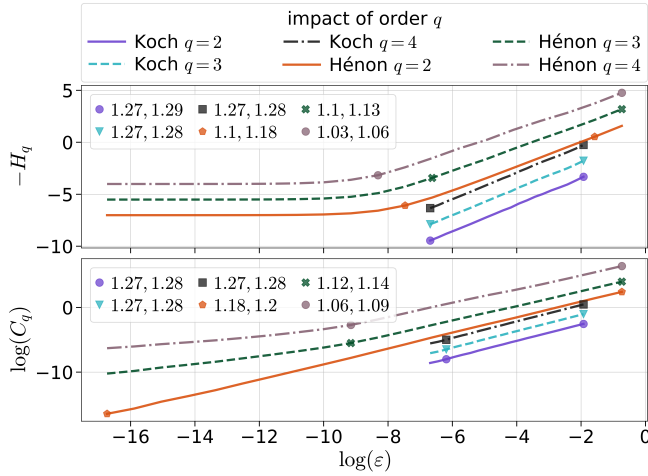


FIG. 4: Impact of order q on the fractal dimension. We used the standard least squares fit for $\log(C)$ as Ref.²⁶ does not discuss $q \neq 2$. The curves have been vertically offset for visual clarity.

we get $\Delta_{\max}^{(C)}(N = 500) \approx 5.4$, however Fig. 3 shows for data generated by a $D = 8$ dimensional Lorenz-96 system that we obtain higher estimates of the dimension from the estimation algorithm (this is true even without the correction of Ref.²⁶). Nevertheless, one should note the relatively small range of magnitudes covered by the $\log(\varepsilon)$. Generally speaking one would want to cover many orders of magnitude before claiming an accurate result for Δ , given that by definition it describes a scaling behavior.

D. q -order dimensions (multi-fractality)

Here we examine how well the estimators capture multi-fractal properties, i.e. the dependence of Δ on q , or the absence of multi-fractality. This dependence on q was discussed in the review by Theiler¹⁰, but we think an even better reference is in the book by Rosenberg⁴⁴. A known theoretical result is that Δ is a non-increasing function of q , $\Delta_{q_2} \leq \Delta_{q_1}$ for $q_2 > q_1$. We will use two examples. The first is the Koch snowflake, which is a uniform fractal and thus its dimension should have no dependence on q whatsoever. The second is the Hénon map, which has a highly singular natural measure, giving the expectation of a clear decrease of Δ with increasing q . The results are in Fig. 4.

Both the entropy and correlation sum approaches perfectly capture the absence of multi-fractality, giving identical curves for all q for the Koch snowflake. For the Hénon map estimates, both methods satisfy the criterion of a decreasing Δ with q . But there is a problem. For the correlation sum method and for $q \neq 2$, the function $\log(C)$ vs. $\log(\varepsilon)$ is no longer a straight line, but is composed of two linear regions with significantly different slope, making the results ambiguous. We could not find anything in the literature about this, and in fact, we could not find a single figure in the literature plotting C_q

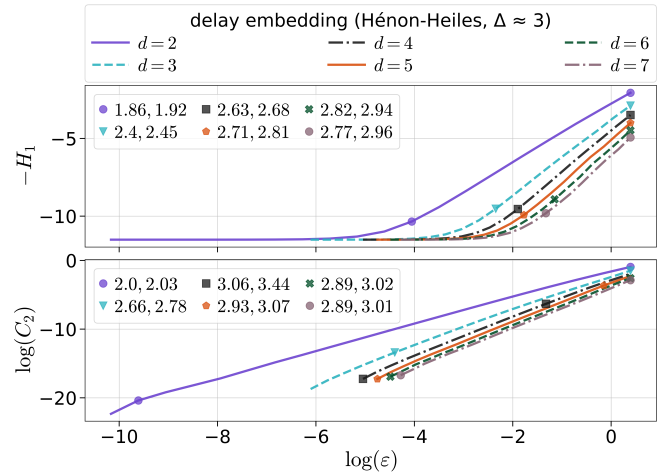


FIG. 5: Effect of different delay embeddings (input dimensionality) on the fractal dimension.

versus ε for $q \neq 2$, even though the correlation sum for $q \neq 2$ is provided in several publications^{5,16,23}. We only found figures reporting directly a value for $\Delta_{q \neq 2}^{(C)}$, without showing how, or where, this was obtained from.

For multi-fractal analysis we are interested in quantifying the most fine properties of the fractal, as we are interested in the singularities of the natural measure. Perhaps then one should obtain the slope of the linear region at the *smallest* ε values, instead of the slope of the linear region covering the largest range of ε . In any case, this is worrisome and indicates that more clarity regarding $C_{q \neq 2}$ must be established in the literature.

E. Delay embedding

This section is examining the impact of varying dimensionality of input data, which is common case when delay-embedding timeseries^{16,45,46}. In principle, provided the condition $d > \Delta_0^{(H)}$ is met, with $d \in \mathbb{N}$ the embedding dimension, then the reconstructed set has the same fractal dimension as the original set the timeseries was recorded from⁴⁷. In Fig. 5 we check how the methods fare with this statement, and how their accuracy decreases with increasing input dimensionality, i.e. embedding dimension.

In Fig. 5 we used a chaotic timeseries from the Hénon-Heiles system. This has $\Delta = 3$ and as such we expect convergence of the fractal dimension estimates to a value around 3 for $d \geq 4$. We see in Fig. 5 that this is indeed the case. Furthermore it seems that $\Delta^{(H)}$ increases its accuracy (in the sense of coming closer to $\Delta = 3$) with increasing d . The same is true for a timeseries from the chaotic Rössler system. For other cases, e.g. a timeseries from a chaotic Lorenz96 system with $D = 4$, which also has $\Delta \approx 3$, we found different results. The accuracy of $\Delta^{(H)}$ decreased drastically with increasing d , while for $\Delta^{(C)}$ it did not. The only universal statement that we can derive from this analysis is that $\Delta^{(C)}$ performs much bet-

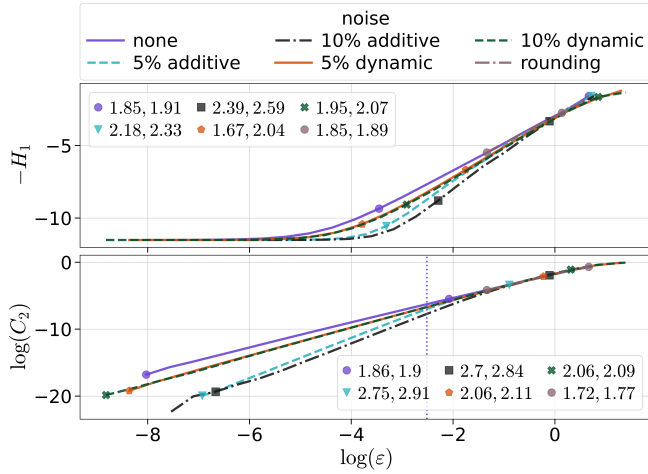


FIG. 6: Impact of noise using the (chaotic) Rössler system as an example. See App. A 4 for a discussion of the vertical dotted line.

ter as the dimensionality of data increases (while keeping data length constant), something that is somewhat already evident from Fig. 2.

F. Noise

This, and the following subsection, are the most important ones for researchers wanting to estimate Δ for real-world data, which are always accompanied with some non-zero amount of noise. As it is well known, the presence of noise in the data makes estimating a fractal dimension harder, as noise has a different (and almost always larger) fractal dimension than that of the original clean data. Figure 6 shows results for various kinds, and amount, of noise added to the chaotic Rössler attractor. On purpose for this plot we have used $\zeta = 1$ (see Sect. IV A), and the standard linear regression method for $\log(C)$, because the logarithmic correction of Ref.²⁶ overestimates $\Delta > 3$ for noisy data (the input dataset is three dimensional and thus cannot have $\Delta > 3$).

We start with the case of additive noise. There it is known that there is some distance ϵ_σ called the “noise level”, below which the slope of $\log(C)$ changes from being the fractal dimension of the chaotic set to that of the noise. This fact can be used to actually estimate the noise level of the data¹⁶. In Fig. 6 we see how quickly this really happens. Even for 5% additive noise, the curve is already dominated with the noise slope (which has $\Delta \approx 3$ for 3-dimensional additive noise). The entropy curve does not have this property, and remains having a single slope throughout (except the saturation part of course), while the slope value is an average between the purely deterministic Δ and that of the noise. On one hand, this may be considered a downside, because it doesn’t allow estimation of noise level. On the other hand, we should note the overwhelming majority of the $\log(C)$ curve is already reflecting the noise. Thus the average slope of the $\log(C)$ curve is much,

much larger than that of H , i.e., it puts much more weight on the noise dimension than the deterministic data. This property of H becomes an advantage for real world data as we will see in the next subsection. These results regarding additive noise are universal and do not depend on the system considered.

For dynamic noise we turned the ODE of the Rössler system into a stochastic differential equation by adding a Wiener process term ηdW in the second equation. For small amount of dynamic noise (which here reflects a proportionality of η with the expected size of the x variable), there is very little change in the fractal dimension. This is even though the actual attractors look very different, and the stochastic version does indeed look noisy (see code online). When one turns up the dynamic noise more, the dynamics collapse and there is no chaotic attractor anymore. So all in all we think the case of dynamic noise cannot be analyzed in a general sense and is system-specific. We also looked at low-resolution data, by rounding Rössler timeseries to 2 digits after the decimal. This obviously decreases the valid ϵ -ranges one can do the computation for (Sect. IV A. For $\Delta^{(C)}$ this also significantly changes the result to a value smaller than “correct”, while for $\Delta^{(H)}$ it has no impact. This means that $\Delta^{(H)}$ performs much better versus rounding, which makes sense given the way it is computed (as long as points are in the same box, it doesn’t matter how close they are to each other).

G. Real world data

In Fig. 7 we show fractal dimension estimates for real world experimental data. We focused specifically in experiments that are relatively clean (large signal to noise ratio) and that the underlying dynamics is well known to display low dimensional deterministic chaos. In Sect. IV B we discuss more what happens with real world data where neither of these two conditions apply. We limited over-sampled experimental data to $N = 50,000$, with sampling of about 10 samples per characteristic timescale. Because of the observations of the previous subsection, we have used $\zeta = 1$ and the standard linear regression method for $\log(C)$ instead of the logarithmic correction of Ref.²⁶.

The datasets are as follows: two electrochemical oscillator datasets (the second being slightly more chaotic than the first) from Ref.¹⁹; time series from a circuit replicating the dynamics of the Shinriki oscillator⁴⁸; the mean field of a network of 28 circuits following Rössler dynamics from Ref.⁴⁹; data from a mechanical double pendulum from Ref.⁵⁰. All experimental timeseries were delay embedded using the recent automated method due to Kraemer et al.¹⁹.

For datasets “Rössler Net” and “electroch. 1” the curve $(\log(\epsilon), \log(C))$ continuously changes its slope instead of having one, or at most two, constant-slope segments. This makes deducing a single fractal dimension invalid, and in fact the numbers quoted in the Figure legend coming from the automated algorithm of Sect. IV A should not be taken seriously. This constant change of slope also happens for “electronch. 2” and “Shinriki” but to a lesser degree. Nevertheless this “constant curving” is something we have not seen before with syn-

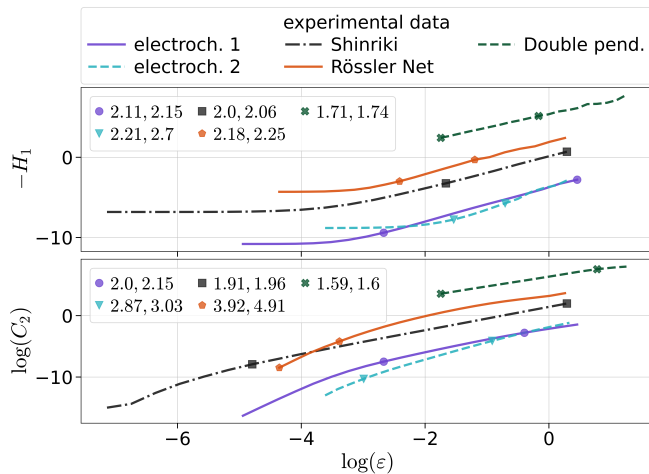


FIG. 7: Fractal dimension estimates for experimental systems known to be underlined by low-dimensional nonlinear dynamics.

thetic data. On the other hand, the entropy-based approach does not suffer from this problem and, besides the expected saturation for small ε , seems to be described quite accurately by a single slope and thus fractal dimension. These results, and with conjunction with the previous subsection, seem to favor $\Delta^{(H)}$ for real data.

IV. COMMON PITFALLS

A. Estimation of slopes and sizes ε

To estimate the value of $\Delta^{(H)}$ or $\Delta^{(C)}$ we need to find the slope of $-H$ or $\log(C)$ versus $\log(\varepsilon)$. This matter is typically resolved in a context-specific manner, where each plot is carefully examined and the “linear region” is decided by the practitioner by eye. This approach cannot work in an objective comparison. Here we formulate an entirely objective and sensible (but not flawless) automated process that is separated into two parts: the choice of which sizes ε to calculate $-H$ or $\log(C)$ for, and how to estimate a linear scaling region from the respective curves. Once the linear scaling region is identified, actually obtaining the fractal dimension is a simple least squares fit.

The range of ε is always decided with generating formula $\varepsilon = e^x$ where x are k linearly spaced values from $\log(\varepsilon_{\min}) + \psi$ to $\log(\varepsilon_{\max}) - \zeta$. I.e., the values of ε are exponentially ranged in base e . ε_{\min} is the smallest inter-point distance existing in the dataset and ε_{\max} the average of the lengths along each of the dimensions of the dataset, and ψ, ζ constants. Unless stated otherwise, we have used $k = 20, \psi = 1, \zeta = 2$ in Sect. III. In essence, we are limiting ε to be one order of magnitude (in base e) larger than the smallest inter-point distance and two orders of magnitude smaller than ε_{\max} . If the resulting ε range does not cover at least two orders of magnitude (common in sparse high dimensional data), we use $\zeta = 0$ in-

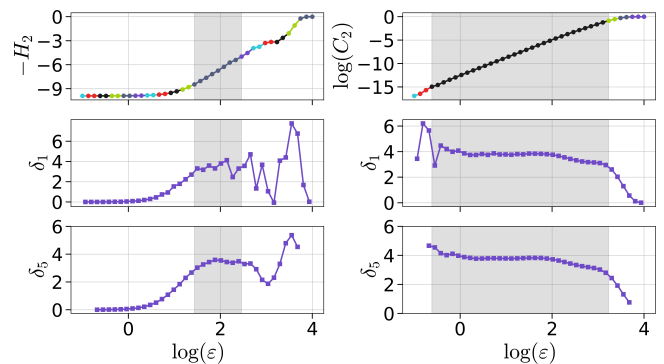


FIG. 8: Demonstration of the algorithm estimating the fractal dimension.

stead. This choice of ε_{\max} brings good enough performance in the box-assisted algorithm for the correlation sum (A 4) but it is not so small as to make the computation meaningless for realistic and/or noisy data. Notice that for most cases the automated fractal dimension estimates are sensitive to k, ζ, ψ . In practice we would recommend to produce several estimates by varying these parameters and obtain the median of Δ .

To estimate the linear region we proceed as follows. We scan the local slopes of each one of the $k - 1$ segments of the curve y vs $\log(\varepsilon)$ starting from the leftmost one (here $y = -H$ or $\log(C)$). If the local slope of the preceding segment is approximately equal to that of the next one with relative tolerance tol , i.e. $|s_{i-1} - s_i| \leq \text{tol} \cdot \max(s_{i-1}, s_i)$, then these two segments belong to the same linear region. We move to the next segment and compare it in the same way with the first segment belonging to the same linear region. When we find a miss-match, we start a new linear region. This way we have segmented the curve y vs $\log(\varepsilon)$ into approximately linear regions. We then choose the linear region which spans the largest amount of the $\log(\varepsilon)$ axis, and label it “the” linear region. We finally perform a least squares fit there and report the 5-95% confidence interval of the fitted slope. In Fig. 8 we visually demonstrate the process. We also compare it with another standard way fractal dimension related plots are presented: the successive local slopes of each point of the curves δ_1 and the same slopes but fitted in a 5-long data window δ_5 . Our linear regions approach is equivalent with finding the largest plateau in the local slopes plots.

Notice that there is a clear pitfall here. This algorithm will deduce a linear region no matter what. In many scenarios this region might be meaningless, being too small to be of actual value, or could even be the scaling of the noise in noisy data, as shown in Sect. III F. So after all, careful consideration of the result is always necessary.

B. Inappropriate data

In this subsection we examine the result of applying the aforementioned methods to inappropriate, or ill-conditioned data which may be non-deterministic or non-stationary. For

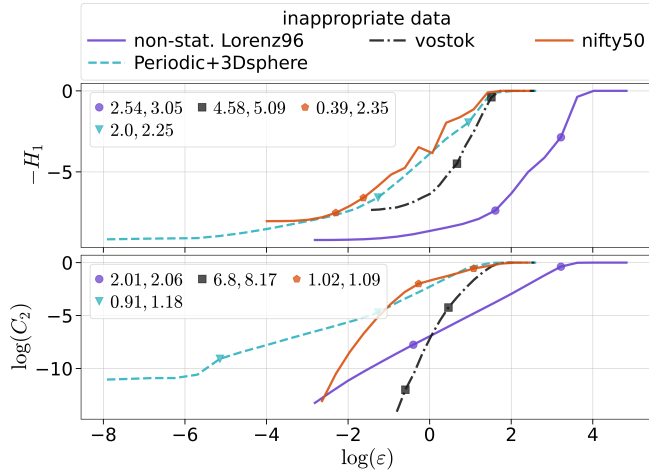


FIG. 9: Calculating the fractal dimension of “inappropriate” data (see text). On purpose here we used $\zeta = 1$ (Sect. IV A), given the considerations of the noise analysis, Sect. III F.

the first dataset we used data from the Lorenz-96 model, with $D = 6$, while having the F parameter increase linearly during the time evolution from 1.0 (periodic motion) to 24.0 (chaotic motion with $\Delta \approx 5$). The second dataset is the concatenation of a periodic trajectory from the Rössler system with noise uniformly distributed on the 3D sphere. Third dataset is a stock market timeseries for the “nifty50” index embedded in 6-dimensional space, which is unlikely to be deterministic. The last dataset is paleoclimate temperature timeseries from the Vostok Ice core, embedded in 8-dimensional space, which is unlikely to be stationary or to accommodate a low-dimensional representation⁵¹.

Generally speaking, in Fig. 9 the curves hint that something is wrong. There is a large miss-match between the estimates of the entropy and correlation sum methods and the curves do not seem to be composed of a single slope. Oddly, for the non-stationary Lorenz96 data, the correlation sum has a clear straight slope with fractal dimension somewhere between the extreme values. The only case where there seems to be a clear slope in both estimators is the Vostok data. Alas, the problem here is that the fractal dimension does not converge but rather increases as the embedded space is increasing. Notice that in all cases our automated algorithm finds a value for Δ nevertheless. This only serves to highlight how careful one should be, and to always plot the curves of H , $\log(C)$.

Although in the literature there exists several tests for non-stationarity using e.g. permutation entropy or other methods, we will now describe a simple, fractal-dimension-based scheme. One can divide the data into m equal parts in two ways: Making m segments of length N/m of successive points, or by choosing every m -th point, each time starting from point 1 to $m - 1$. For these subsets, the same fractal dimension estimation is done. If there is non-stationarity, the first kind of selection will show significantly different estimates across its sub-datasets, while the second will show approximately the same estimates.

C. A note on surrogate timeseries

Surrogate timeseries have been recommended by Theiler et al. in the early 90s⁵² as a mean to test for nonlinearity in noisy timeseries. It was suggested there that a discriminatory statistic for the test can be the fractal dimension computed via the correlation sum. That requires a bit of care. If the algorithm we described here, see eq. (3), is used, the user risks estimating the fractal dimension of the noise (already existing in the original data) instead of the “underlying deterministic nonlinear dynamics data” (if any exist), thus invalidating the hypothesis testing approach in the first place. Other discriminatory statistics should be used instead, see⁵³ for example.

If the fractal dimension is chosen as a discriminatory statistic nevertheless, we propose the following alternatives for computing it: (i) use Takens’ estimator (Sect. A 6) with the empirically good estimate $\epsilon_{\max} = 0.25\text{std}(x)$ with x the original timeseries. Because Takens’ estimator performs a maximum likelihood estimation instead of a linear fit, and thus considers *all* regions of the correlation sum up to some ϵ_{\max} , it produces an “average” fractal dimension of the noise and the underlying data. Or (ii) do a least squares fit to estimate the slope of the *entire curve* of $\log(C)$ vs. $\log(\epsilon)$ using the full limits we describe in Sect. IV A, without attempting to estimate a linear region. It should be clear, however, that the Takens estimator is used in this context (just) as a discriminating statistics and its results must not be interpreted as meaningful dimension estimates.

V. CONCLUSIONS

In this paper we have analyzed in quantitative detail all practically relevant fractal dimension estimators we found in the literature. It is clear, as it was before this work, that estimating a fractal dimension is not an easy task. Focusing on only a single number can mislead. The best practice we feel is to calculate several versions of Δ , from different methods and with varying the parameters of each method (including the range of ϵ) and produce e.g., a median of the results. Furthermore, plotting of the appropriate quantities (H , $\log(C)$ versus a length scale ϵ) can hint whether the methods are applied at inappropriate data.

Our conclusions are as follows. From all these estimators, the oldest entropy-based, and a modified box-assisted correlation-sum based are on average the most robust, most straightforward to compute, most accurate, and least ambiguous estimators. This, and our detailed analysis and comparison of the Appendix A, highlights the importance of sharing a code implementation when proposing a new algorithm, so that such comparisons can be done during the peer review process. Here we provide open source and performant implementations for every algorithm. Using these implementations we found that for synthetic data the correlation sum method clearly performs better than the entropy one. The correlation sum method can also be used to detect the “noise radius”, as e.g. illustrated by Kantz and Schreiber¹⁶. Unfortunately for real data this is more of a downside, making the estima-

tion ambiguous due to an almost continuous change of slope (Fig. 7). So we conclude that for real experimental data the entropy method performs better, as it only has single slope. We had difficulties making sense of correlation sum for order $q \neq 2$, even though it has been mentioned several times in the literature. As such, we suggest that when treating multifractality, the entropy method should be preferred. In Sect. III C we saw that, provided one has clean data, it is still quite sensible to attempt and estimated a fractal dimension from ultra-small datasets even if they are high dimensional. Lastly, we note that the numeric performance of the entropy-based method is massively faster than the correlation sum one and also scales better for increasing N (see end of App. A 4).

To keep this paper within sensible limits, we have used a relatively small subset of possible systems and real-world data. Nevertheless we believe that the results we present are robust, and have been applied to other datasets not shown. We further motivate usage of the online code that reproduces this paper, for cross-checking results with all kinds of input data and dynamical systems.

As an outlook, we believe there is still some future research to be done regarding estimating fractal dimensions. Besides the Lyapunov dimension, every single estimator we have used in this work disregards the time-ordering information. While by definition this information is not important for these estimators, perhaps here is a way to make a more powerful estimator by using this discarded information of the time-ordering of the points in the dataset.

Appendix A: Algorithms for estimating a fractal dimension

1. Optimized histograms for arbitrary ε

Here we describe an optimized method to calculate histograms, which to our knowledge neither has been published before, nor we could find a faster method that works for arbitrary ε . The process has memory allocation scaling of $D \cdot N$ and performance scaling of $D \cdot N \log(N)$, neither of which depends on ε . The processes is as follows. Every point in the dataset is first mapped to its corresponding bin via the operation $\mathbf{b}_i = \lfloor (\mathbf{x}_i - \mathbf{x}_{\min}) / \varepsilon \rfloor$, where \mathbf{x}_{\min} is a vector containing the minimum value of the dataset along each dimension and $\lfloor \cdot \rfloor$ is the floor operation. The resulting \mathbf{b} (N in total) are then sorted with a quick sorting algorithm, which results in all equal \mathbf{b}_i being successive to each other. We then count the successive occurrences of equal $\mathbf{b}_i \equiv \mathbf{b}_{i+1}$, which gives the amount of points present in the corresponding bin and move on to the next bin (there are no actual bins being created in memory, a bin is conceptually defined as the group of successively equal \mathbf{b}_i). Dividing by the total amount of points gives the probabilities that can then be plugged into Eq. (1).

2. The Box-Counting Algorithm by Molteno

This box-counting algorithm for the generalized dimension was introduced by Molteno²² as an improvement for the

method introduced by Grassberger⁵⁴. It claims to be of order $D \cdot N$. The algorithm partitions the data into boxes and counts the number of points in each box to retrieve the probabilities p_i necessary to calculate the generalized dimension $\Delta^{(H)}$. The faster runtime of the algorithm is due to the use of integer manipulations for the division of the data points into boxes.

To perform these manipulations, all data values are converted to unsigned integers. These are calculated by finding the maxima \mathbf{x}_{\max} and minima \mathbf{x}_{\min} in each dimension to then identify the dimension that covers the largest range X .

$$\mathbf{x}_{\text{Int}}(\mathbf{x}) = \left\lfloor 2^{N_{\text{bits}}-1} \left(\frac{\mathbf{x} - \mathbf{x}_{\min}}{X} \right) \right\rfloor, \quad (\text{A1})$$

where N_{bits} is the bit size of the unsigned integer type that was used and $\lfloor \cdot \rfloor$ is the floor function.

The first box contains all indices to the array that stores the data points, where a box refers to an array of indices. The boxes are subsequently partitioned, until the mean number of points per filled box falls below a threshold k_0 , recommended by Molteno to be 10.

The k th step of partitioning divides the previous box into 2^D new boxes with the dimension of the data D . For a data point \mathbf{x} , the index i of its new box is calculated as

$$i = \sum_{j=1}^D ((x_j \gg (N_{\text{bits}} - k)) \& 1) \cdot 2^j. \quad (\text{A2})$$

Here \gg is the logical shift operation, shifting the bit representation of the first value to the right by the second value, $\&$ is the bit-wise “and” operation. Thereby $(x_j \gg (N_{\text{bits}} - k)) \& 1$ translates to checking whether the bit at position $N_{\text{bits}} - k + 1$ is one. In a cycle of partition, all boxes that contain more than one data point are split up and empty ones are deleted. To retrieve the probabilities p_i , the number of data points contained in each box is counted and divided by the total number of data points.

The algorithm provides exponentially scaled sets of values, that suit the approximation of the limit in Eq. (2) and it only needs to compute the operation (A2) $D \cdot N$ times per partitioning process. The main disadvantage is the static box size choice. It works well for low-dimensional data sets, but for larger dimensions the number of boxes increases exponentially with dimension, thereby increasing the number of points necessary to calculate the dimension exponentially. This drastically limits the yielded ε range the algorithm is applied over, and for some sets makes the computation of low accuracy or even straight-out impossible. Given how incredibly fast our histogram algorithm already is (all H curves in this paper took on average 0.1 seconds to compute), we saw no reason to use the Molteno method. Also, the Molteno method does not allow the user to decide ε values, making it less flexible.

3. Correlation sum

The original correlation sum can be calculated as given in (3). Since the calculation time scales with N^2 this method

is exceptionally slow for high N . Notice that the version of the q -order correlation sum given in Eqn. (3) differs from the version proposed by Kantz and Schreiber¹⁶ in the exponent of $1/(q-1)$. If the q -order correlation given by Kantz and Schreiber is called $\bar{C}_q(\varepsilon)$, it scales as $\bar{C}_q(\varepsilon) \sim \varepsilon^{(q-1)\Delta_q^{(C)}}$, then $\bar{C}_q(\varepsilon)^{1/(q-1)} = C_q(\varepsilon) \sim \varepsilon^{\Delta_q^{(C)}}$ and both versions are equal.

4. The Box and Prism assisted Correlation sum

Theiler²⁴ proposed an improvement over the calculation of the correlation dimension by Grassberger and Procaccia⁵⁵ that divides the data into boxes before calculating the distances between points. Thereby the number of distance calculations is reduced and the scaling changes from N^2 to something faster (which depends on the box size r_0). After division into boxes the formula given in (3) is used to calculate the correlation sum, therefore an extension to the q -order correlation sum is possible.

The integer representations of the boxes $b(\mathbf{x})$ with sidelength r_0 can be calculated by

$$b(\mathbf{x}) = \left\lfloor \frac{\mathbf{x} - \mathbf{x}_{\min}}{r_0} \right\rfloor \quad (\text{A3})$$

for each point \mathbf{x} and the minimum of each dimension \mathbf{x}_{\min} . This method is based upon section (A 1), as Theiler does not specify a method for the calculation of the boxes. The permutations needed to sort all representations in lexicographic order are calculated with a quick sort algorithm. The representations have the same ordering as the points they were calculated with, therefore sorting the points into boxes reduces to the iteration through the permutations and searching for changing integer representations. If the integer representation changes, all previous permutations are stored in an array.

For a point inside a box, there may be points outside the box that are within the given distance of the point. Therefore the neighboring boxes w.r.t. the current box also have to be found and checked. The distances between the points in the box and its neighbors are calculated as given in Eq. (3). The first sum runs over all points of the initial box and the second sum uses all points in the box and adjacent boxes.

A point of criticism for this algorithm is its poor runtime for higher dimensions. The advantage of distributing the points into boxes beforehand diminishes as the number of boxes increases considerably with dimension. To reduce the amount of boxes, Theiler proposed a prism algorithm, where only the first P dimensions are used to distribute the data into boxes. These new boxes, where P sides are of sidelength r_0 and the other $D-P$ sides cover the whole range, are called prisms. The best choice given by Theiler is $P = 0.5 \log_2 N$ and should be used when D exceeds $0.75 \log_2 N$.

According to Theiler, the size of the boxes r_0 can be computed as

$$r_0 = R(2/N)^{1/\Delta^{(C)}}, \quad (\text{A4})$$

where R is the size of the chaotic attractor and the dimension $\Delta^{(C)}$ is estimated by computation of the correlation sum for

\sqrt{N} points. Since these points are chosen randomly, the estimated dimension and in consequence the box size and even the final dimension can vary strongly. A down side is that for some sets the proposed box size can drop below the minimum interpoint distance of the set. Furthermore, our tests showed an irregular output value of r_0 with differences as high as two orders of magnitude for two box size estimates on the Hénon map.

Bueno-Orovio and Pérez-García²⁵ proposed a different, and more stable, algorithm for the calculation of the optimal box size r_0 . They optimized the expected calculation times for the optimal number of filled boxes to

$$\eta_{\text{opt}} \approx N^{2/3} \left[\frac{3^{\Delta^{(C)}} - 1}{3^{D/P} - 1} \right]^{1/3}.$$

D/P is the number of dimensions used for the boxing, D for boxes and P for prisms. Introducing the effective length of the chaotic attractor $\ell = r_\ell \eta_\ell^{1/\Delta^{(C)}}$ and solving $\eta_{\text{opt}} = (\ell/r_0)^{\Delta^{(C)}}$ for the box size r_0 yields

$$r_0 = \frac{\ell}{\eta_{\text{opt}}^{1/\Delta^{(C)}}}. \quad (\text{A5})$$

ℓ is the effective length, r_ℓ is the box size used to calculate the effective length with $r_\ell = R/10$ and η_ℓ is the number of filled boxes in case of the effective length. η_ℓ is calculated by distributing $N/10$ points into boxes of size r_ℓ . The dimension $\Delta^{(C)}$ used for the calculation of r_0 , η_{opt} and ℓ is again estimated by computation of the correlation sum for \sqrt{N} points.

The box size estimator still varies in its choice of box size but shows fluctuations with smaller amplitude than the Theiler estimator. The choice of a box size smaller than the smallest interpoint distance only occurs for high dimensional data sets with a low number of points. Furthermore, Bueno-Orovio and Pérez-García chose a prism dimension of always $P = 2$ (for $D > 2$). However a prism dimension of 2 can result in box size estimates smaller than the minimal interpoint distance for high dimensional datasets with comparably low size. In this paper we used $P = 2$ but we have different r_0 , see below.

The main benefit of a small r_0 is that it makes the computations much faster. Unfortunately, both suggestions, and especially that of Ref.²⁵, often fail in practice. They give much too small r_0 values and for data with any amount of noise whatsoever this value is well below the noise radius. This is displayed in Fig. 6. The vertical dotted line shows the r_0 estimated by Eq. (A5) (the calculation of C would be limited up to this r_0). It is so small, that even for only 2.5% additive noise the computation would only show the noise dimension and no hint of the deterministic (and smaller) slope of $\log(C)$ vs. $\log(\varepsilon)$. That is why in this paper we decided to use the box-assisted version for better performance, but with $r_0 = \varepsilon_{\max}/e$ or $|e^2$ as discussed in Sect. IV A. The performance is not too bad, e.g. for the typical data lengths considered here computing the entire C curve takes about a minute on an average computer. Notice that even with the optimized-for-performance r_0 of Ref.²⁵, the entropy-method is still massively faster (in fact it is even faster than just computing r_0).

5. Fixed-Mass correlation dimension

The correlation dimension stems from the assumption, that the probabilities p_i scale as $\sum_i \left(p_i^q / \delta_i^{-(q-1)D_q} \right) \sim 1$ for $\varepsilon \rightarrow 0$ with δ_i being the diameter of the partition. In most methods that compute the dimension, the diameter is fixed and the probabilities are defined by the set. The fixed mass algorithm does the opposite: the probabilities are fixed by defining $p_i = n/N$, where n is a chosen number of points and N the total number of points in the set. The diameter is chosen to include n points. Rewritten the scaling then assumes the form of Eq. (A6)

$$\overline{(r^{(j)})^{-\tau}} = \frac{1}{M} \sum_{i=1}^M (r_i^{(j)})^{-(q-1)\Delta_q} \sim N^{q-1} \frac{\Gamma(j+1-q)}{\Gamma(j)}. \quad (\text{A6})$$

$\overline{(r^{(j)})^{-\tau}}$ is the mean of all radii that contain j points, M is the number of points of the set considered for the calculation, Γ is the gamma function. Eq. (A6) is not solvable for Δ_q in general. Eq. (A7) can be obtained from Eq. (A6) from the limit $q \rightarrow 1$ and applying L'Hôpital's rule.

$$\Delta_1 \overline{\log r^{(j)}} \sim \Psi(j) - \log N. \quad (\text{A7})$$

Ψ is the digamma function, $\Psi(x) = d \log \Gamma(x) / dx$. With a general form that is not solvable this algorithm is restricted to $q = 1$. We also did not find any performance or accuracy benefits on using this version instead of the more established correlation sum approach, so we did not consider it further for the main comparison.

6. Takens' Estimator

The estimator introduced by Takens⁷ aims to estimate the correlation dimension using the method of maximum likelihood estimation (MLE)⁵⁶. From m interpoint-distances $\rho_j < \varepsilon_{\max}$, one can estimate the correlation dimension as

$$\Delta^{(T)} = - \frac{m-1}{\sum_{j=1}^m \log \frac{\rho_j}{\varepsilon_{\max}}}. \quad (\text{A8})$$

The derivation of this formula starts with the assumption that $\exists \varepsilon_{\max} > 0$, so that $\forall 0 \leq \varepsilon \leq \varepsilon_{\max}$, the correlation sum

$$C(\varepsilon) = c \varepsilon^{\Delta^{(T)}} \quad \text{exactly}, \quad (\text{A9})$$

without any higher order terms, for some proportionality constant c .

The transformed variable $y_i = -\log(\rho_i / \varepsilon_{\max})$ is distributed exponentially with parameter $\Delta^{(T)}$. The log-likelihood-function of this distribution is given by

$$l(\Delta^{(T)}; \{y_i\}) = \log L(\Delta^{(T)}; \{y_i\}) = m \log \Delta^{(T)} - \Delta^{(T)} \sum_{j=1}^m y_j.$$

l is then maximised with respect to $\Delta^{(T)}$ to obtain the most likely value of the correlation dimension. As Takens noted

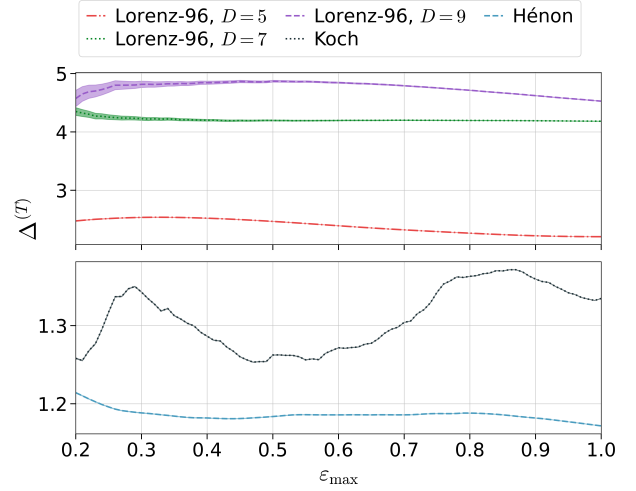


FIG. 10: Dependency of $\Delta^{(T)}$ for different systems on the parameter ε_{\max} . The shaded 5%-95% confidence intervals around the curves are not visible in most cases. Clearly, the variation of $\Delta^{(T)}$ over different values of ε_{\max} exceeds the confidence intervals.

correctly, just taking the maximum of l is biased^{7,27}, which can be easily corrected by writing

$$\Delta^{(T)} = \frac{m-1}{\underset{\text{correction}}{m} \frac{m}{\sum_{j=1}^m y_j}} = \frac{m-1}{\sum_{j=1}^m y_j}.$$

For a Gaussian distributed random variable, the log-likelihood function is a parabola, that at 1σ has fallen by 0.5 from its maximum and at 2σ by 2. By invariance⁵⁷, this is also the case for a non-Gaussian random variable, letting us easily estimate the variance of $\Delta^{(T)}$.

When testing the algorithm and its dependency on ε_{\max} on different dynamical systems, we found that the variation of $\Delta^{(T)}$ exceeds the confidence intervals at any fixed ε_{\max} for low dimensional systems.

These variations occur because for the estimation, it is assumed that Eq. (A9) holds. Thus, the estimated $\Delta^{(T)}$ and its confidence intervals are of no use as long as the validity of the assumption (A9) is not known.

While Takens' estimator does not provide a significant advantage in the precise estimation of the fractal dimension, compared to correlation-sum based methods, it can be useful in the case of surrogate timeseries as described in Sect. IV C.

7. "Improved Estimator" for the Correlation Dimension by Judd

Judd's "improved estimator" for the correlation dimension^{28,29} also uses MLE. To account for deviations from uniform scaling, it allows a polynomial a of degree t , so that the assumed correlation sum is

$$C(\varepsilon) \approx \varepsilon^{\Delta^{(J)}} (a_0 + a_1 \varepsilon + \dots + a_t \varepsilon^t). \quad (\text{A10})$$

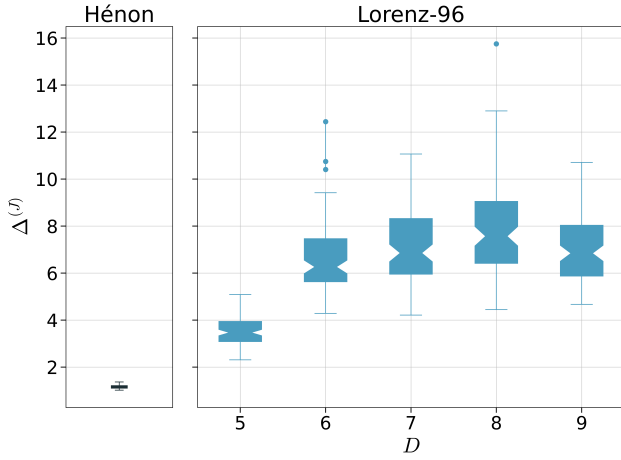


FIG. 11: Estimates of $\Delta^{(J)}$ for different dynamical systems. For each box, 100 different samples have been drawn from a trajectory. Each individual sample contained 100 points. The degree of the polynomial was $\deg(a) = 1$.

It is stated that a degree $t \leq 2$ is "usually sufficient".

The estimator performs a binned maximum likelihood estimation of $\Delta^{(J)}$ alongside the coefficients of the polynomial. Judd therefore introduces a logarithmic binning, where the bins are defined by $B_0 = [\varepsilon_0, \infty)$, $\varepsilon_i = \lambda^i \varepsilon_0$ and $B_i = [\varepsilon_i, \varepsilon_{i-1})$ for $i > 0$ and $\lambda < 1$. The parameter ε_0 is called the *cutoff* and $w = \log(1/\lambda)$ the bin width. Now, the probability of observing a distance in bin B_i becomes $p_i = P_i - P_{i+1}$, with

$$P_i = \left(\frac{\varepsilon_i}{\varepsilon_0}\right)^{\Delta^{(J)}} \left[a_0 + a_1 \left(\frac{\varepsilon_i}{\varepsilon_0}\right) + \dots + a_t \left(\frac{\varepsilon_i}{\varepsilon_0}\right)^t \right]$$

If the bin contents b_i are distributed multinomially, the negative log-likelihood function for the bin contents $\{b_i\}$ is

$$l(\{b_i\}; \Delta^{(J)}, a) = - \sum_i b_i \log p_i + C, \quad (\text{A11})$$

which must be minimized under the constraints

$$\sum_i p_i = 1 \quad \text{and} \quad p_i > 0. \quad (\text{A12})$$

Eq. (A11) does not necessarily only have one minimum because it depends on $t+2$ parameters and must be minimized numerically.

The optimal bin width for the estimator w minimizes

$$\log w + \log \binom{n}{b_1 \dots b_m} + \log \binom{n+m+1}{m}, \quad (\text{A13})$$

where m is the index of the last bin for which the bin content $b_m \neq 0$ and n is the number of considered interpoint distances. Because the computation time of Eq. (A13) becomes unreasonably large for large numbers of distances, the estimator is restricted to small sample sizes.

Once the optimal bin width is found, the cutoff ε_0 is chosen as the right edge of the fullest bin of the histogram. All bins to the right of this bin are joined to form $B_0 = [\varepsilon_0, \infty)$.

The minimization of Eq. (A11) is subject to two difficulties that are already noted by Judd. First, an optimizer cannot understand the idea that the exponential $\varepsilon^{\Delta^{(J)}}$ is the essence of the model, while the polynomial is only a device to correct for deviations from the scaling law. Second, the optimizer is highly sensitive to the initial condition of the optimization, which could be reduced by a tailored optimizer⁵⁸, but still one can observe a very broad distribution of $\Delta^{(J)}$ over different samples of a long trajectory, especially for higher-dimensional systems, as is shown in Fig. 11.

Due to these problems, we decided not to include the estimator in the main comparison.

8. Dimension from Lyapunov exponents

In Sect. II C we described the Lyapunov dimension $\Delta^{(L)}$ due to Kaplan and Yorke. We do not have anything to add here regarding $\Delta^{(L)}$, but we want to mention Ref.³² by Chlouverakis and Sprott. They suggest that instead of a linear interpolation to the sum of λ_i , a polynomial interpolation should be done instead. However, as we found no theoretical foundation for this proposal, we decided to skip it (and we also did not notice any significant improvement with the numeric results).

9. Mean return times

According to the Poincaré recurrence theorem, any trajectory within an ergodic set⁵⁹ will return arbitrarily often and arbitrarily close to any neighborhood in the ergodic set. We represent this neighborhood as a hypersphere of radius ε , centered at some point \mathbf{x}_0 in the ergodic set, and define as γ the mean return time to this hypersphere. Then one expects that $\log(\gamma) \approx -\Delta^{(\gamma)} \log(\varepsilon)$ with $\Delta^{(\gamma)}$ the fractal dimension, as estimated from the mean return times. A more formal discussion of this fact, and explicit connection with the natural measure of the ergodic set and the fractal dimension obtained via the generalized entropy (2) is given by Theiler¹⁰. Earliest reference we found using return times to estimate fractal dimensions was Ref.³⁰.

Unfortunately, the method using mean return times is not recommended at all. A fundamental limitation is that knowledge of the dynamic rule f is necessary, otherwise the results of the method for measured data are too inaccurate to be considered seriously. Even for known rule f , the method converges slowly (numerically). Furthermore, it provides an estimate of the local dimension around the point of return, similarly with the point-wise dimension. Thus, it has to be further averaged over several state-space points, requiring several orders of magnitude more computation time than the correlation sum method or the Lyapunov dimension method. Lastly, we found its numeric output (not shown, see online repository) to be quite far from the results of the correlation dimension and thus we do not consider it accurate enough.

Appendix B: Software implementations and code base

The work done in this paper, as well as the figures produced, are also available as a fully reproducible code base, which can be found on GitHub⁶⁰. It is written in the Julia language⁶¹, and is using the software: DynamicalSystems.jl²⁰, DifferentialEquations.jl⁶², BenchmarkTools.jl⁶³, GLM.jl, LsqFit.jl, and DrWatson⁶⁴. Figures were produced with the matplotlib library⁶⁵. All methods, with the exception of Judd’s algorithm, are implemented, documented, and tested, in DynamicalSystems.jl²⁰. We made the implementations easy to use, yet optimized. The following code is a simple example of calculating $\Delta_2^{(C)}$ with DynamicalSystems.jl and the Julia language:

```
using DynamicalSystems
# some input data (chaotic Roessler system)
ds = Systems.roessler()
X = trajectory(ds, 1000.0; Ttr = 1e3)
# Estimate correlation sum
es = estimate_boxsizes(X) # Sect. IV. A
Cs = boxed_correlationsum(X, es; q = 2)
# find and fit largest linear region
_, Delta = linear_region(log.(es), log.(Cs))
```

Appendix C: Dynamic rules of known systems

All dynamical systems used for generating data are listed in Table. III.

REFERENCES

- ¹B. B. Mandelbrot, *The fractal geometry of nature*, Vol. 2 (WH freeman New York, 1982).
- ²K. Falconer, *Fractal Geometry Mathematical Foundations and Applications* (2003).
- ³E. Ott, “Attractor dimensions,” *Scholarpedia* **3**, 2110 (2008), revision #91015.
- ⁴P. Grassberger and I. Procaccia, “Characterization of strange attractors,” *Physical Review Letters* **50**, 346–349 (1983).
- ⁵P. Grassberger and I. Procaccia, “Measuring the strangeness of strange attractors,” *Physica D: Nonlinear Phenomena* **9**, 189–208 (1983).
- ⁶P. Frederickson, J. L. Kaplan, E. D. Yorke, and J. A. Yorke, “The liapunov dimension of strange attractors,” *Journal of Differential Equations* **49**, 185–207 (1983).
- ⁷F. Takens, “On the numerical determination of the dimension of an attractor,” in *Dynamical Systems and Bifurcations*, edited by B. L. J. Braaksma, H. W. Broer, and F. Takens (Springer Berlin Heidelberg, Berlin, Heidelberg, 1985) pp. 99–106.
- ⁸G. Paladin and A. Vulpiani, “Anomalous scaling laws in multifractal objects,” *Physics Reports* **156**, 147–225 (1987).
- ⁹D. Ruelle, *Chaotic Evolution and Strange Attractors* (Cambridge University Press, 1989).
- ¹⁰J. Theiler, “Statistical precision of dimension estimators,” *Phys. Rev. A* **41**, 3038–3051 (1990).
- ¹¹D. A. Russell, J. D. Hanson, and E. Ott, “Dimension of strange attractors,” *Physical Review Letters* **45**, 1175–1178 (1980).
- ¹²E. Ott, *Chaos in Dynamical Systems* (Cambridge University Press, 2012) arXiv:1011.1669.
- ¹³C. Grebogi, S. W. McDonald, E. Ott, and J. A. Yorke, “Final state sensitivity: An obstruction to predictability,” *Physics Letters A* **99**, 415–418 (1983).
- ¹⁴S. Banerjee, “Coexisting attractors, chaotic saddles, and fractal basins in a power electronic circuit,” *IEEE Transactions on Circuits and Systems I: Fundamental Theory and Applications* **44**, 847–849 (1997).
- ¹⁵T. Tel and M. Gruiz, *Chaotic Dynamics, An Introduction Based on Classical Mechanics* (Cambridge University Press, 2007).
- ¹⁶H. Kantz and T. Schreiber, *Nonlinear Time Series Analysis*, 2nd ed. (Cambridge University Press, 2003).
- ¹⁷H. D. I. Abarbanel, *Analysis of Observed Chaotic Data* (Springer New York, 1996).
- ¹⁸E. Bradley and H. Kantz, “Nonlinear time-series analysis revisited,” *Chaos* **25** (2015), 10.1063/1.4917289, arXiv:1503.07493.
- ¹⁹K. H. Kraemer, G. Datsis, J. Kurths, I. Z. Kiss, J. L. Ocampo-Espindola, and N. Marwan, “A unified and automated approach to attractor reconstruction,” *New Journal of Physics* **23**, 033017 (2021).
- ²⁰G. Datsis, “Dynamicalsystems.jl: A julia software library for chaos and nonlinear dynamics,” *Journal of Open Source Software* **3**, 598 (2018).
- ²¹R. Lopes and N. Betrouni, “Fractal and multifractal analysis: A review,” *Medical Image Analysis* **13**, 634–649 (2009).
- ²²T. C. A. Molteno, “Fast o(n) box-counting algorithm for estimating dimensions,” *Phys. Rev. E* **48**, R3263–R3266 (1993).
- ²³P. Grassberger, “Grassberger-Procaccia algorithm,” *Scholarpedia* **2**, 3043 (2007), revision #91330.
- ²⁴J. Theiler, “Efficient algorithm for estimating the correlation dimension from a set of discrete points,” *Phys. Rev. A* **36**, 4456–4462 (1987).
- ²⁵A. Bueno-Orovio and V. M. Pérez-García, “Enhanced box and prism assisted algorithms for computing the correlation dimension,” *Chaos, Solitons & Fractals* **34**, 509 – 518 (2007).
- ²⁶J. C. Sprott and G. Rowlands, “Improved correlation dimension calculation,” *International Journal of Bifurcation and Chaos in Applied Sciences and Engineering* **11**, 1865–1880 (2001).
- ²⁷S. Borovkova, R. Burton, and H. Dehling, “Consistency of the takens estimator for the correlation dimension,” *Ann. Appl. Probab.* **9**, 376–390 (1999).
- ²⁸K. Judd, “An improved estimator of dimension and some comments on providing confidence intervals,” *Physica D: Nonlinear Phenomena* **56**, 216 – 228 (1992).
- ²⁹K. Judd, “Estimating dimension from small samples,” *Physica D: Nonlinear Phenomena* **71**, 421 – 429 (1994).
- ³⁰M. H. Jensen, L. P. Kadanoff, A. Libchaber, I. Procaccia, and J. Stavans, “Global universality at the onset of chaos: Results of a forced rayleigh-bénard experiment,” *Physical Review Letters* **55**, 2798–2801 (1985).
- ³¹J. L. Kaplan and J. A. Yorke, “Chaotic behavior of multidimensional difference equations,” in *Functional Differential Equations and Approximation of Fixed Points*, edited by H.-O. Peitgen and H.-O. Walthier (Springer Berlin Heidelberg, Berlin, Heidelberg, 1979) pp. 204–227.
- ³²K. E. Chlouverakis and J. C. Sprott, “A comparison of correlation and Lyapunov dimensions,” *Physica D: Nonlinear Phenomena* **200**, 156–164 (2005).
- ³³A. Rényi, “On the dimension and entropy of probability distributions,” *Acta Mathematica Academiae Scientiarum Hungaricae* **10**, 193–215 (1959).
- ³⁴P. Grassberger, “Generalized dimensions of strange attractors,” *Physics Letters A* **97**, 227 – 230 (1983).
- ³⁵H. Hentschel and I. Procaccia, “The infinite number of generalized dimensions of fractals and strange attractors,” *Physica D: Nonlinear Phenomena* **8**, 435 – 444 (1983).
- ³⁶J. Theiler, “Spurious dimension from correlation algorithms applied to limited time-series data,” *Physical Review A* **34**, 2427–2432 (1986).
- ³⁷Wikipedia contributors, “Kaplan-yorke conjecture — Wikipedia, the free encyclopedia,” (2020), [Online; accessed 12-June-2020].
- ³⁸F. Ledrappier, “Some relations between dimension and lyapounov exponents,” *Communications in Mathematical Physics* **81**, 229–238 (1981).
- ³⁹I. Shimada and T. Nagashima, “A Numerical Approach to Ergodic Problem of Dissipative Dynamical Systems,” *Progress of Theoretical Physics* **61**, 1605–1616 (1979).
- ⁴⁰G. Benettin, L. Galgani, A. Giorgilli, and J.-M. Strelcyn, “Lyapunov Characteristic Exponents for Smooth Dynamical Systems and for Hamiltonian Systems ; a Method for Computing All of Them , Part 1 : Theory .” *Mechanica* **15**, 9–20 (1980).
- ⁴¹U. Parlitz, “Estimating lyapunov exponents from time series.” in *Chaos detection and predictability*, Lecture Notes in Physics, Vol. 915, edited by

System	Dynamical rule	Initial conditions	Parameters
Hénon map	$x_{n+1} = 1 - ax_n^2 + y_n, \quad y_{n+1} = bx_n$	(0.08, 0.12)	$a = 1.4, b = 0.3$
Kaplan-Yorke map	$x_{n+1} = 2x_n \% 1, \quad y_{n+1} = \lambda y_n + \cos(4\pi x_n)$	(0.15, 0.2)	$\lambda = 0.2$
Towel map	$x_{n+1} = 3.8x_n(1 - x_n) - 0.05(y_n + 0.35)(1 - 2z_n),$ $y_{n+1} = 0.1((y_n + 0.35)(1 + 2z_n) - 1)(1 - 1.9x_n),$ $z_{n+1} = 3.78z_n(1 - z_n) + by_n$	(0.085, -0.121, 0.075)	
Hénon-Heiles	$\dot{x} = p_x, \dot{y} = p_y, \dot{p}_x = -x - 2xy, \dot{p}_y = -y - (x^2 - y^2)$	(0, -0.25, 0.42081, 0)	
Coupled logistic maps	$u_{n+1}^{(i)} = 4v_n^{(i)}(1 - v_n^{(i)}),$ $v_n^{(i)} = u_n^{(i)} + k(u_n^{(i-1)} - 2u_n^{(i)} + u_n^{(i+1)})$	(0.1, ..., 0.9)	$k = 0.1$
Rössler	$\dot{x} = -y - z, \quad \dot{y} = x + ay, \quad \dot{z} = b + z(x - c)$	(0.1, -0.2, 0.1)	$a = b = 0.2, c = 5.7$ periodic parameters: $a = b = 0.2, c = 3$
Lorenz-96	$\dot{x}_i = (x_{i+1} - x_{i-2})x_{i-1} - x_i + F$	$(j \times 0.1 \text{ for } j \in 0 \dots D - 1) \quad F = 24$	

TABLE III: Description of various systems considered in this paper.

- C. H. Skokos, G. A. Gottwald, and J. Laskar (Springer, Berlin; Heidelberg, 2016) pp. 1–34.
- ⁴²J. P. Eckmann and D. Ruelle, “Fundamental limitations for estimating dimensions and Lyapunov exponents in dynamical systems,” *Physica D: Nonlinear Phenomena* **56**, 185–187 (1992).
- ⁴³Note that Ref.⁴² argues exclusively for data coming from delay embedding of a timeseries. However we see no reason, neither conceptual nor technical, why the same argument shouldn’t hold for data sampled directly from the multi-dimensional attractor. Also note that their equation 2 is incorrectly typed, writing η instead of \mathcal{N} .
- ⁴⁴E. Rosenberg, “Generalized dimensions and multifractals,” in *Fractal Dimensions of Networks* (Springer International Publishing, Cham, 2020) pp. 325–364.
- ⁴⁵N. H. Packard, J. P. Crutchfield, J. D. Farmer, and R. S. Shaw, “Geometry from a time series,” *Physical Review Letters* **45**, 712–716 (1980).
- ⁴⁶F. Takens, “Detecting strange attractors in turbulence,” in *Dynamical Systems and Turbulence, Warwick 1980*, edited by D. Rand and L.-S. Young (Springer Berlin Heidelberg, Berlin, Heidelberg, 1981) pp. 366–381.
- ⁴⁷T. Sauer, J. Yorke, and M. Casdagli, “Embedology,” *J. Stat. Phys.* **65**, 579–616 (1991).
- ⁴⁸M. Shinriki, M. Yamamoto, and S. Mori, “Multimode oscillations in a modified van der pol oscillator containing a positive nonlinear conductance,” *Proceedings of the IEEE* **69**, 394–395 (1981).
- ⁴⁹V. P. Vera-Ávila, R. Sevilla-Escoboza, A. A. Lozano-Sánchez, R. R. Rivera-Durón, and J. M. Buldú, “Experimental datasets of networks of nonlinear oscillators: Structure and dynamics during the path to synchronization,” *Data in brief* **28**, 105012–105012 (2019).
- ⁵⁰A. Asseman, T. Kornuta, and A. Ozcan, “Learning beyond simulated physics,” in *Modeling and Decision-making in the Spatiotemporal Domain Workshop* (2018).
- ⁵¹P. Grassberger, “Do climatic attractors exist?” *Nature* **323**, 609–612 (1986).
- ⁵²J. Theiler, S. Eubank, A. Longtin, B. Galdrikian, and J. Doynne Farmer, “Testing for nonlinearity in time series: the method of surrogate data,” *Physica D: Nonlinear Phenomena* **58**, 77–94 (1992).
- ⁵³G. Lancaster, D. Iatsenko, A. Pidde, V. Ticcinelli, and A. Stefanovska, “Surrogate data for hypothesis testing of physical systems,” *Physics Reports* **748**, 1–60 (2018).
- ⁵⁴P. Grassberger, “An optimized box-assisted algorithm for fractal dimensions,” *Physics Letters A* **148**, 63 – 68 (1990).
- ⁵⁵P. Grassberger and I. Procaccia, “Measuring the strangeness of strange attractors,” *Physica D: Nonlinear Phenomena* **9**, 189 – 208 (1983).
- ⁵⁶A. Mallet, “A maximum likelihood estimation method for random coefficient regression models,” *Biometrika* **73**, 645–656 (1986), <https://academic.oup.com/biomet/article-pdf/73/3/645/694101/73-3-645.pdf>.
- ⁵⁷P. W. Zehna *et al.*, “Invariance of maximum likelihood estimators,” *Annals of Mathematical Statistics* **37**, 744 (1966).
- ⁵⁸The optimization is split into to parts, where first $\Delta^{(j)}$ is optimized for a fixed a , and afterwards the coefficients of a are optimized. This process is repeated until a convergence of the entire parameter vector, $(\Delta^{(j)}, a)^T$ is observed.
- ⁵⁹For the purposes of this paper we assume all invariant sets to be ergodic. While not always true, it is sufficiently accurate for our practical focus.
- ⁶⁰G. Datseris, “Fractal Dimension code base,” <https://github.com/datseris/fractalDimension>, accessed: 2021-09-13.
- ⁶¹J. Bezanson, A. Edelman, S. Karpinski, and V. B. Shah, “Julia: A fresh approach to numerical computing,” *SIAM Review* **59**, 65–98 (2017).
- ⁶²C. Rackauckas and Q. Nie, “DifferentialEquations.jl – a performant and feature-rich ecosystem for solving differential equations in julia,” *The Journal of Open Research Software* **5** (2017), 10.5334/jors.151, exported from <https://app.dimensions.ai> on 2019/05/05.
- ⁶³J. Chen and J. Revels, “Robust benchmarking in noisy environments,” (2016), arXiv:1608.04295 [cs.PF].

- ⁶⁴G. Datseris, J. Isensee, S. Pech, and T. Gál, “Drwatson: the perfect sidekick for your scientific inquiries,” *Journal of Open Source Software* **5**, 2673 (2020).
- ⁶⁵J. D. Hunter, “Matplotlib: A 2d graphics environment,” *Computing in Science & Engineering* **9**, 90–95 (2007).
- ⁶⁶E. N. Lorenz, “Dimension of weather and climate attractors,” *Nature* **353**, 241–244 (1991).
- ⁶⁷F. Camastra, “Data dimensionality estimation methods: a survey,” *Pattern Recognition* **36**, 2945–2954 (2003).
- ⁶⁸C. Song, L. K. Gallos, S. Havlin, and H. A. Makse, “How to calculate the fractal dimension of a complex network: the box covering algorithm,” *Journal of Statistical Mechanics: Theory and Experiment* **2007**, P03006–P03006 (2007).
- ⁶⁹K. E. Chlouverakis and J. Sprott, “A comparison of correlation and Lyapunov dimensions,” *Physica D: Nonlinear Phenomena* **200**, 156 – 164 (2005).
- ⁷⁰H. von Koch, *Sur une courbe continue sans tangente obtenue par une construction geometrique elementaire* (Norstedt & soner, 1904).
- ⁷¹L. Pontrjagin and L. Schnirelmann, “Sur une propriete metrique de la dimension,” *The Annals of Mathematics* **33**, 156 (1932).
- ⁷²“Documentation of DynamicalSystems.jl,” <https://juliadynamics.github.io/DynamicalSystems.jl/dev/>, accessed: 2021-09-13.